Implications of a 125 GeV Higgs scalar for the LHC supersymmetry and neutralino dark matter searches

Howard Baer,[1,*] Vernon Barger,[2,†] and Azar Mustafayev[3,‡]

[1]*Department of Physics and Astronomy, University of Oklahoma, Norman, Oklahoma 73019, USA*
[2]*Department of Physics, University of Wisconsin, Madison, Wisconsin 53706, USA*
[3]*William I. Fine Theoretical Physics Institute, University of Minnesota, Minneapolis, Minnesota 55455, USA*

(Received 2 February 2012; published 12 April 2012)

The ATLAS and CMS collaborations have reported an excess of events in the $\gamma\gamma$, $ZZ^* \to 4\ell$ and WW^* search channels at an invariant mass $m \simeq 125$ GeV, which could be the first evidence for the long-awaited Higgs boson. We investigate the consequences of requiring $m_h \simeq 125$ GeV in both the minimal supergravity and 2-parameter nonuniversal Higgs supersymmetric models. In minimal supergravity, large values of trilinear soft breaking parameter $|A_0|$ are required, and universal scalar $m_0 \gtrsim 0.8$ TeV is favored so that we expect squark and slepton masses typically in the multi-TeV range. This typically gives rise to an "effective supersymmetric" type of sparticle mass spectrum. In this case, we expect gluino pair production as the dominant sparticle creation reaction at LHC. For $m_0 \lesssim 5$ TeV, the superpotential parameter $\mu \gtrsim 2$ TeV and $m_A \gtrsim 0.8$ TeV, greatly restricting neutralino annihilation mechanisms. These latter conclusions are softened if $m_0 \sim 10$–20 TeV or if one proceeds to the 2-parameter nonuniversal Higgs model. The standard neutralino abundance tends to be far above WMAP-measured values unless the neutralino is Higgsino-like. We remark upon possible nonstandard (but perhaps more attractive) cosmological scenarios which can bring the predicted dark matter abundance into accord with the measured value, and discuss the implications for direct and indirect detection of neutralino cold dark matter.

DOI: 10.1103/PhysRevD.85.075010 PACS numbers: 12.60.Jv, 14.80.Da, 14.80.Ly

I. INTRODUCTION

Recently, the ATLAS and CMS experiments have performed a combined search [1] for the standard model (SM) Higgs boson $H_{\rm SM}$ using 1–2.3 fb^{-1} of integrated luminosity with the result that the region 141 GeV $< m_{H_{\rm SM}} <$ 476 GeV is now excluded as a possibility at 95% C.L. Even more recently, using the full data sample in excess of 5 fb^{-1} per experiment collected in 2011, the ATLAS [2] and CMS [3] collaborations have reported excesses in the Higgs search $\gamma\gamma$, $ZZ^* \to 4\ell$ and $WW^* \to 2\ell$ channels with reconstructed invariant mass $m(\gamma\gamma) \sim m(4\ell) \sim$ 125 GeV. The combined statistical significance lies at the 2.5σ level. These latest results might be construed as the first emerging direct evidence of the Higgs boson. Indeed, these new Higgs search results are consistent with the combined LEP2 [4] and Tevatron precision electroweak analyses [5] which favor the existence of a Higgs boson with mass not much beyond the LEP2 limit of $m_{H_{\rm SM}} > 114.4$ GeV.

While the putative $m_h \sim 125$ GeV signal is consistent with SM expectations, it is rather stunning that it is also well in accord with expectations from supersymmetric (SUSY) models, where the window of possible Higgs masses m_h is far smaller. In the minimal supersymmetric standard model (MSSM), the Higgs sector consists of two doublet fields H_u and H_d, which after the breaking of electroweak symmetry, result in the five physical Higgs bosons: two neutral CP-even scalars h and H, a neutral CP-odd pseudoscalar A, and a pair of charged scalars $H^\pm$ [6]. At tree level, the value of m_h is bounded by $M_Z|\cos 2\beta|$, where $\tan\beta \equiv v_u/v_d$ is the ratio of Higgs field vacuum expectation values. Including radiative corrections, which depend on various sparticle masses and mixings that enter the h-boson self-energy calculation, one finds instead that $m_h \lesssim 135$ GeV [7]. In fact, using $\sim$1 fb^{-1} of data in summer 2011, ATLAS [8] and CMS [9] had already reported some excess of WW^* events. In Ref. [10], such events had been shown to favor a rather high mass light Higgs scalar h, with mass in the $m_h \sim$ 125–130 GeV range, and with large scalar masses m_0 and large trilinear soft breaking terms $A_0 \sim \pm 2m_0$ [10].

Over most of the MSSM parameter space, the lighest Higgs boson h is nearly SM-like so that SM Higgs search results can also be directly applied to h (for exceptions, see Ref. [11]). A calculation of the light (heavy) scalar Higgs boson mass at 1-loop level using the effective potential method gives

$$m_{h,H} = \frac{1}{2}[(m_A^2 + M_Z^2 + \delta) \mp \xi^{1/2}], \tag{1.1}$$

where m_A is the mass of the CP-odd pseudoscalar A and

*baer@nhn.ou.edu
†barger@pheno.wisc.edu
‡mustafayev@physics.umn.edu

$$\xi = [(m_A^2 - M_Z^2)\cos 2\beta + \delta]^2 + \sin^2 2\beta (m_A^2 + M_Z^2)^2. \tag{1.2}$$

The radiative corrections can be approximated as follows:

$$\delta = \frac{3g^2 m_t^4}{16\pi^2 M_W^2 \sin^2\beta} \log\left[\left(1 + \frac{m_{\tilde{t}_L}^2}{m_t^2}\right)\left(1 + \frac{m_{\tilde{t}_R}^2}{m_t^2}\right)\right]. \tag{1.3}$$

Thus, in order to accommodate a value of $m_h \sim 125$ GeV, we anticipate rather large values of top squark soft masses $m_{\tilde{t}_{L,R}}$ typically at least into the few-TeV range.

For our calculation of m_h, we include the full third generation contribution to the effective potential, including all sparticle mixing effects [12]. The effective Higgs potential, $V_{\rm eff}$, is evaluated with all running parameters in the $\overline{DR}$ renormalization scheme evaluated at the scale choice $Q_{\rm SUSY} = \sqrt{m_{\tilde{t}_1} m_{\tilde{t}_2}}$, i.e. the mean top squark mass scale. Of particular importance is that the t, b, and τ Yukawa couplings are evaluated at the scale $Q_{\rm SUSY}$ using 2-loop MSSM renomalization group equations and including full 1-loop MSSM radiative corrections [13]. Evaluating $V_{\rm eff}$ at this (optimized) scale choice then includes the most important two-loop effects [14]. This calculation procedure has been embedded in the ISAJET mass spectra program ISASUGRA [15], which we used for the present work. We note that just a few GeV theory error is expected in our m_h calculation. Also, it should be noted that our value of m_h is typically a couple GeV below the corresponding Feyn Higgs [16] calculation, mainly due to the fact that we are able to extract and use the two-loop $\overline{DR}$ Yukawa couplings including 1-loop threshold corrections in our calculation of radiative corrections to m_h. Our calculation of m_h agrees well with results from SUSPECT, SOFTSUSY, and SPHENO codes [17].

Our goal in this paper is to calculate the implications of a 125 GeV light Higgs scalar h for supersymmetry searches at LHC, and for direct and indirect neutralino dark matter searches. In Sec. II, we examine implications of a 125 GeV light Higgs scalar in the paradigm minimal supergravity (mSUGRA) model [18]. In Sec. III, we examine implications in the more general 2-parameter nonuniversal Higgs model (NUHM2). In Sec. IV, we examine implications of a 125 GeV light Higgs scalar for $(g-2)_\mu$, BF$(b \to s\gamma)$, BF$(B_s \to \mu^+\mu^-)$ and for direct and indirect searches for neutralino cold dark matter (CDM). In Sec. V, we present our conclusions.

II. IMPLICATIONS OF $m_h = 125$ GeV IN THE MSUGRA MODEL

Our first goal is to examine the implications of a 125 GeV light Higgs scalar for the paradigm mSUGRA model. The well-known parameter space is given by

$$m_0, \quad m_{1/2}, \quad A_0, \quad \tan\beta, \quad \text{sign}(\mu). \tag{2.1}$$

The mass of the top quark also needs to be specified and we take it to be, throughout this paper, $m_t = 173.3$ GeV in accord with the Tevatron results [19].

We begin by plotting contours of m_h in the m_0 vs $m_{1/2}$ plane in Fig. 1(a) for $A_0 = 0$ and $\tan\beta = 10$, with $\mu > 0$ (as favored by the muon magnetic moment anomaly [20]). The gray shaded region leads to a stable tau-slepton and so is excluded by cosmological constraints on long-lived charged relics. The red shaded region is excluded by lack of appropriate radiative electroweak symmetry breaking.

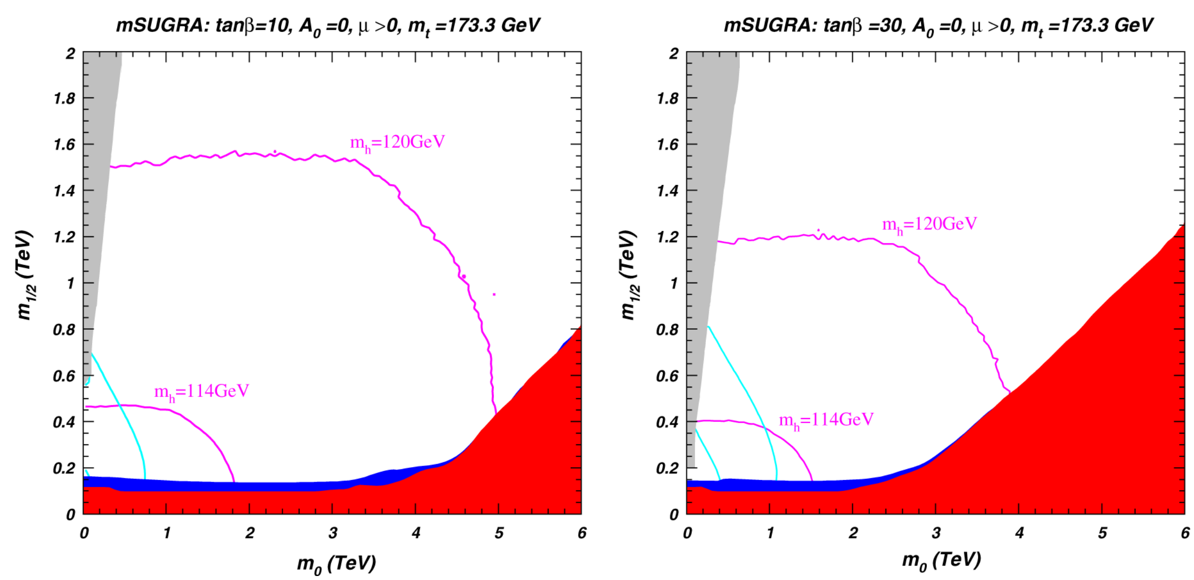

FIG. 1 (color online). Contours of $m_h = 114$ and 120 GeV (magenta) in the m_0 vs $m_{1/2}$ plane of mSUGRA model for $A_0 = 0$, $\tan\beta = 10$ and 30 and $\mu > 0$ with $m_t = 173.3$ GeV. The region consistent with $(g-2)_\mu$ measurement at 3σ is between the blue contours. The gray and the red shaded regions are excluded by the stau LSP and the lack of EWSB, respectively. The blue-shaded region is excluded by the LEP2 chargino search.

The blue-shaded region is excluded by LEP2 searches [21], and indicates where $m_{\tilde{W}_1} < 103.5$ GeV. The lower-left magenta contour denotes $m_h = 114$ GeV, while the outer contour beginning around $m_{1/2} \sim 1.5$ TeV denotes $m_h = 120$ GeV. When possible, we also plot a third contour with $m_h = 125$ GeV. However, in this case, $m_h < 125$ GeV in the entire plane shown. A similar situation occurs in Fig. 1(b), for $A_0 = 0$ and $\tan\beta = 30$. Indeed, for $A_0 = 0$, one must move to exceedingly high values of $m_{1/2} \sim m_0 \sim 10$ TeV to gain regions with $m_h \sim 125$ GeV. Such mSUGRA parameter values place both gluino and squark masses in the 20 TeV range, way beyond the LHC reach with $\sqrt{s} = 7$ TeV [22] or even 14 TeV [23]. We may thus expect that the m_0 vs $m_{1/2}$ planes of mSUGRA are excluded for $A_0 = 0$.

The radiative corrections to m_h depend sensitively upon the top squark mixing parameter $A_t - \mu \cot\beta$, where A_t is the weak-scale trilinear soft breaking parameter and μ is the superpotential Higgsino mass term. For fixed $\tan\beta$, the mixing is largely controlled by A_t, which depends on the grand unified theory (GUT) scale value A_0. Thus, in Fig. 2(a), we plot the value of m_h generated versus variation in A_0 for fixed other mSUGRA parameters $m_0 = 4$ TeV, $m_{1/2} = 0.5$ TeV, $\mu > 0$, and $\tan\beta = 10$, 30, 45, and 55. We see indeed that at $A_0 = 0$, the value of m_h is nearly minimal, while for $A_0 \sim \pm 2m_0$, the value of m_h is maximized, and indeed can be pushed into the 125 GeV range. The gaps in the curves around $A_0 \sim 0$ occur due to a breakdown of radiative electroweak symmetry breaking (EWSB) (beyond the hyperbolic branch/focus point (HB/FP) region [24]), while the curves terminate at very large $|A_0|$ due to generation of tachyonic top squarks. In Fig. 2(b), we show the top squark mass $m_{\tilde{t}_1}$ versus A_0 for the same parameter choices as in Fig. 2(a). Here, we see the highly mixed $\tilde{t}_1$ state is nearly at its lightest value when m_h is maximal.

Inspired by the large values of m_h for $A_0 \sim \pm 2m_0$, we plot the mSUGRA plane for $A_0 = \pm 2m_0$ with $\tan\beta = 10$ and 30 in Fig. 3. In Fig. 3(a) with $A_0 = -2m_0$ and $\tan\beta = 10$, we see that the $m_h = 125$ GeV contour roughly independent of $m_{1/2}$, and lying nearly along the line at $m_0 \simeq 2.5$ TeV. In Fig. 3(b), for $A_0 = -2m_0$ but $\tan\beta = 30$, the $m_h = 125$ GeV contour is again nearly independent of $m_{1/2}$, this time lying nearly along the line $m_0 \simeq 2$ TeV. In Fig. 3(c), for $A_0 = +2m_0$ and $\tan\beta = 10$, we see the $m_h = 125$ GeV contour has moved out to much higher m_0 values ~6–10 TeV. In this case, with such large m_0 values, we expect a SUSY mass spectrum of the "effective SUSY" variety, wherein scalar masses are in the multi-TeV range, and well-beyond the LHC reach [25]. However, gauginos can still be quite light, and may be accessible to LHC SUSY searches. This situation persists in Fig. 3(d), where we keep $A_0 = +2m_0$, but take $\tan\beta = 30$.

To make our results more general, we scan over the range

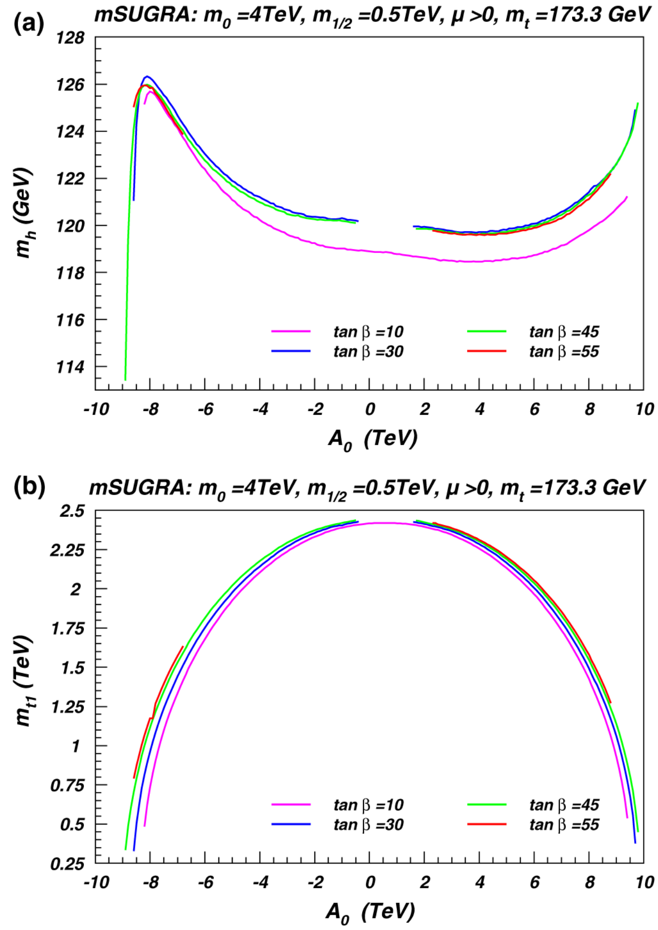

FIG. 2 (color online). Plot of (a) m_h vs A_0 in the mSUGRA model for $m_0 = 4$ TeV, $m_{1/2} = 0.5$ TeV, $\mu > 0$ and various values of $\tan\beta$. In frame (b), we show $m_{\tilde{t}_1}$ vs A_0 versus A_0 for the same parameter choices. Curves terminate due to the lack of EWSB or because top squark becomes tachyonic.

$$m_0\colon 0 \rightarrow 5 \text{ TeV} \quad \text{(blue points)};$$
$$m_0\colon 0 \rightarrow 20 \text{ TeV} \quad \text{(orange points)}, \tag{2.2}$$

$$m_{1/2}\colon 0 \rightarrow 2 \text{ TeV}, \tag{2.3}$$

$$A_0\colon -5m_0 \rightarrow +5m_0, \tag{2.4}$$

$$\tan\beta\colon 5 \rightarrow 55. \tag{2.5}$$

We employed ISAJET 7.81 to generate 30K random points in the above parameter space, requiring only that $m_{\tilde{W}_1} > 103.5$ GeV. The radiative electroweak symmetry breaking is maintained and the lightest supersymmetric particle (LSP) is required to be the lightest neutralino $\tilde{Z}_1$. We only scan over positive μ values so that we do not stray more than 3σ away from the measured value of the muon anomalous magnetic moment, $(g-2)_\mu$ [20].

A plot of the calculated m_h values from ISASUGRA is shown versus the various mSUGRA parameters in Fig. 4.

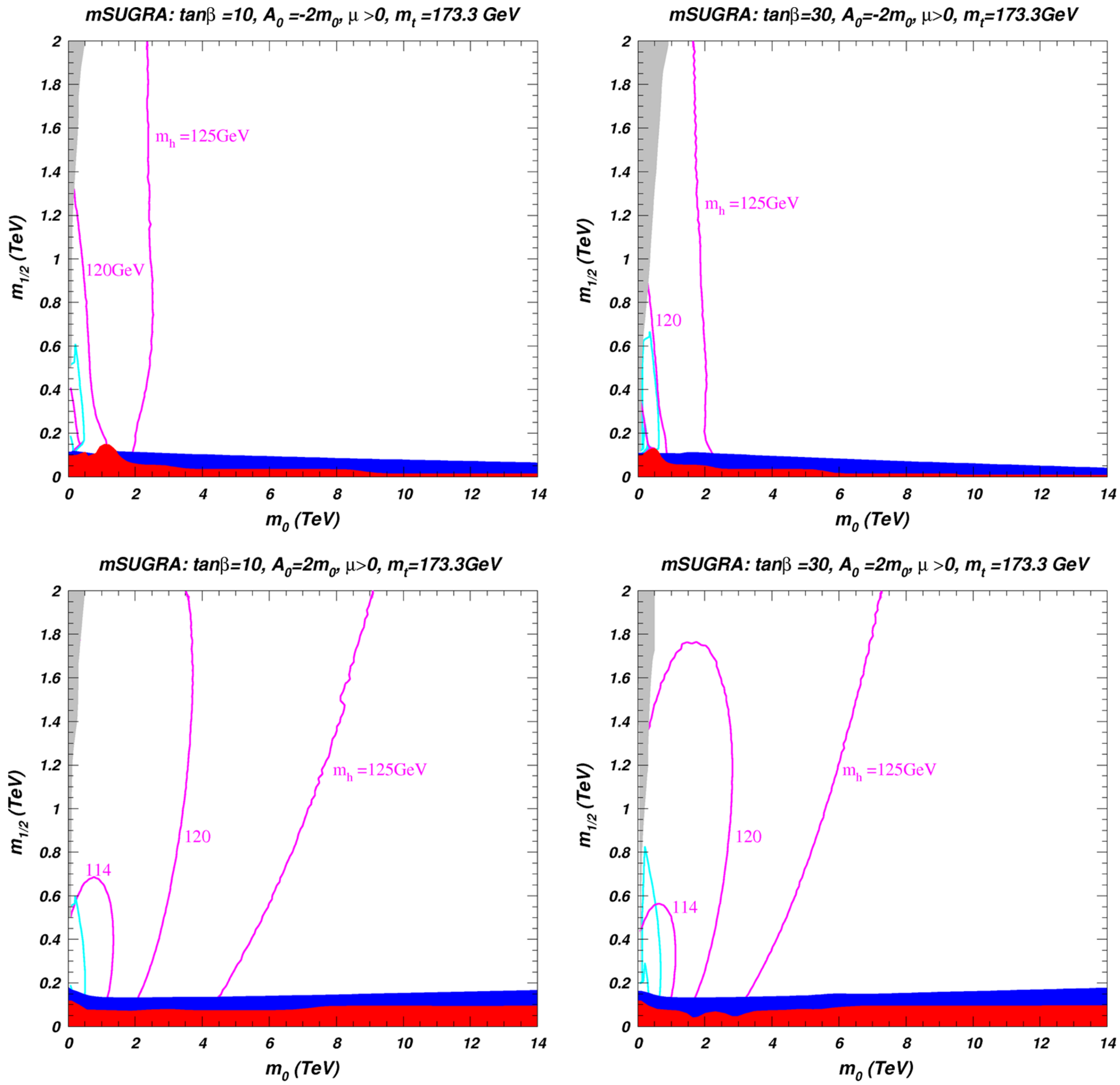

FIG. 3 (color online). Contours of $m_h = 114$, 120, and 125 GeV in the m_0 vs $m_{1/2}$ plane of mSUGRA model for $A_0 = \pm 2m_0$, $\tan\beta = 10$ and 30, and $\mu > 0$ with $m_t = 173.3$ GeV. The color coding is the same as in Fig. 1.

Points with $m_0 < 5$ TeV are denoted by blue, while points with 5 TeV $< m_0 < 20$ TeV are denoted by orange. We see from Fig. 4(a) that $m_0 \gtrsim 0.8$ TeV is required, and much larger m_0 values in the multi-TeV range are favored based on density of points. In Fig. 4(b), we see that $m_h \simeq 125$ GeV does not favor any particular $m_{1/2}$ value, although slightly higher m_h values are allowed for very low $m_{1/2}$ (as in Ref. [10]). In Fig. 4(c), we see that $|A_0| \lesssim 1.8m_0$ is essentially *ruled out in the mSUGRA model* in the case where $m_0 < 5$ TeV. Also—while the entire range $A_0 < -1.8m_0$ is allowed by our scan for $m_0 < 5$ TeV—for positive A_0, only the narrow range $A_0 \sim 2m_0$ seems allowed. If we allow $m_0 > 5$ TeV, then still $A_0 \sim 0$ is excluded, but now the allowed range drops to $A_0/m_0 \lesssim 0.3$. In Fig. 4(d), we see that nearly the entire range of $\tan\beta$ is allowed, except for the small region with $\tan\beta \lesssim 6$. A second scan (not shown here) using $3 < \tan\beta < 60$ confirmed this result to be robust.

For the mSUGRA model, both $|\mu|$ and m_A are derived parameters. Figure 4(e) shows that $m_h \simeq 125$ GeV translates into the requirement $|\mu| > 2$ TeV for $m_0 < 5$ TeV. *This result highly restricts the possibility of light mixed bino-Higgsino CDM as would occur in the lower $m_{1/2}$ portion of the HB/FP region* [24]. However, if we allow $m_0 \sim 5$–20 TeV, then low values of $|\mu|$ become allowed. Basically, taking A_0/m_0 to be large pushes the HB/FP region out to very large, multi-TeV values of m_0; in this case, we can regain a region containing a neutralino $\tilde{Z}_1$ of mixed bino-Higgsino variety, which is characteristic of the HB/FP region, and which has a low value of the neutralino relic density, $\Omega_{\tilde{Z}_1} h^2 \lesssim 0.1277$. In Fig. 4(f), we see that m_A is favored to be $m_A \gtrsim 0.8$ TeV, which also restricts the

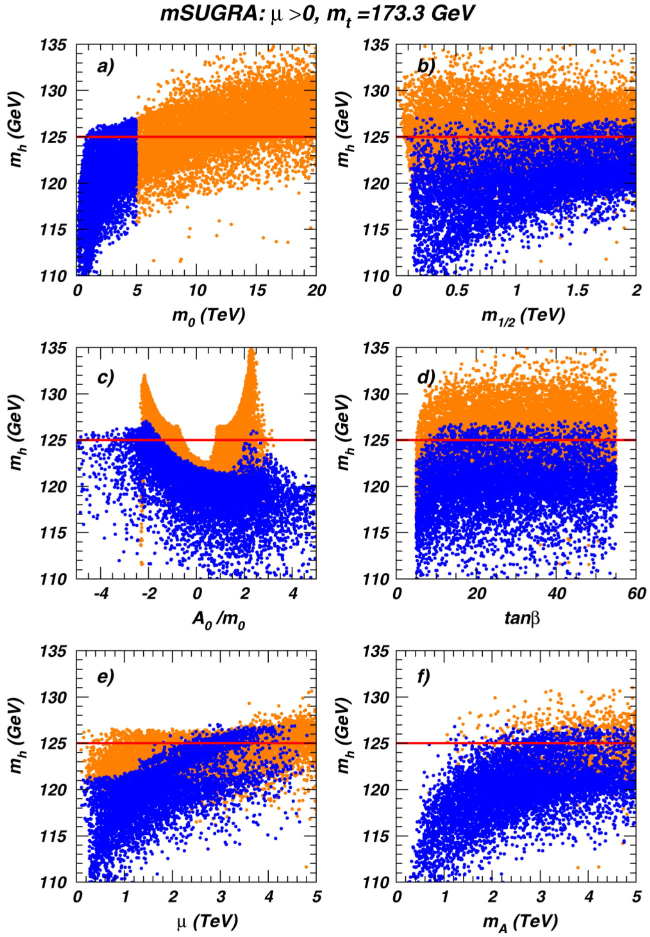

FIG. 4 (color online). Lightest Higgs boson mass versus various parameters from the mSUGRA model for $\mu > 0$ with $m_t = 173.3$ GeV. Blue points denote $m_0 < 5$ TeV, while orange points allow m_0 values up to 20 TeV.

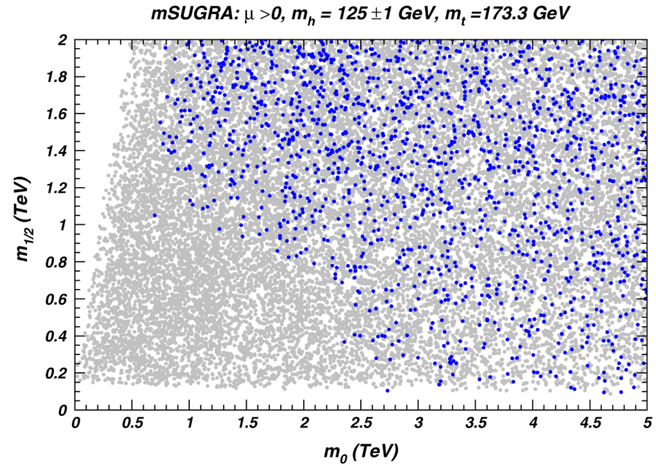

FIG. 5 (color online). Plot of points from general scan over mSUGRA model in m_0 vs $m_{1/2}$ plane for $\mu > 0$ with $m_t = 173.3$ GeV. Gray points require neutralino LSP and $m_{\tilde{W}_1} > 103.5$ GeV, while blue points additionally require $m_h = 125 \pm 1$ GeV.

possibility of A-funnel dark matter annihilation [26] for rather light $\tilde{Z}_1$ states, since this possibility requires $m_{\tilde{Z}_1} \simeq m_A/2$.

In Fig. 5, we show points from our general scan over mSUGRA parameters (gray points for any value of m_h) and with $m_h = 125 \pm 1$ GeV (blue points) in the m_0 vs $m_{1/2}$ plane. Here the most remarkable result is that the entire low m_0 and low $m_{1/2}$ region is actually excluded by requiring a large value of $m_h \sim 125$ GeV. This bound is even more restrictive than the ATLAS and CMS direct search for SUSY limits [27,28] which only extend up to $m_{1/2} \sim 0.5$ TeV.

In Fig. 6 we show the distribution of the mSUGRA scan points in the m_0 vs A_0/m_0 plane. Here, we see the blue points with $m_h = 125 \pm 1$ GeV only allow for positive $A_0 \sim 2m_0$ as long as $m_0 \gtrsim 3$–4 TeV. Alternatively, large negative A_0 values seem much more likely, and allow for m_0 values somewhat below 1 TeV.

To gain perspective on the sort of sparticle masses we expect in mSUGRA with $m_h = 125 \pm 1$ GeV, we plot in Fig. 7 various physical mass combinations along with the value of the superpotential μ parameter. Gray points require $\tilde{Z}_1$ to be the LSP, $\tilde{W}_1$ to satisfy the lower bound of 103.5 GeV from LEP2 and has no restriction on the Higgs boson mass m_h, while blue points require $m_h = 125 \pm 1$ GeV. Green points have in addition $\Omega_{\tilde{Z}_1} h^2 < 0.0941$, while red points have $0.0941 < \Omega_{\tilde{Z}_1} h^2 < 0.1277$, which is the 3σ range of the WMAP-7 [29]. In Fig. 7(a), we see that first/second generation squarks—typified by the $\tilde{u}_L$ mass—are required to be $m_{\tilde{q}} \gtrsim 2$ TeV. Meanwhile, the light top squark $\tilde{t}_1$ usually has $m_{\tilde{t}_1} \sim m_{\tilde{q}}/2$, although it can range as low as a few hundred GeV. In Fig. 7(b), we see a wide range of $\tilde{t}_1$ and $\tilde{g}$ masses are allowed, although if $\tilde{t}_1$ is very light—$m_{\tilde{t}_1} \lesssim 1$ TeV is favored by fine-tuning arguments—then $m_{\tilde{g}}$ is typically

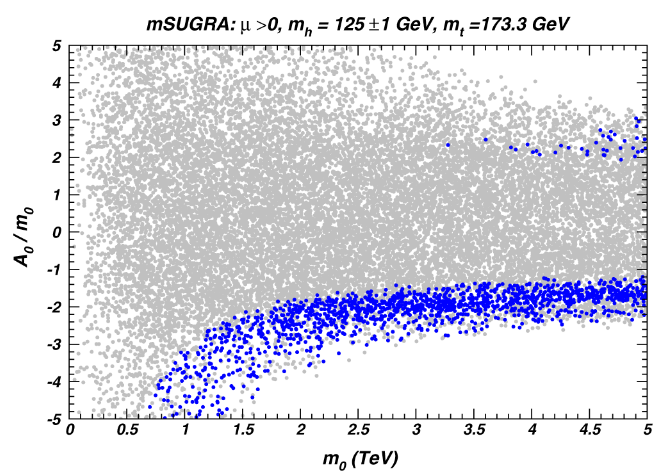

FIG. 6 (color online). Plot of points from general scan over mSUGRA model in m_0 vs A_0/m_0 plane for $\mu > 0$ with $m_t = 173.3$ GeV. The color coding is the same as in Fig. 5.

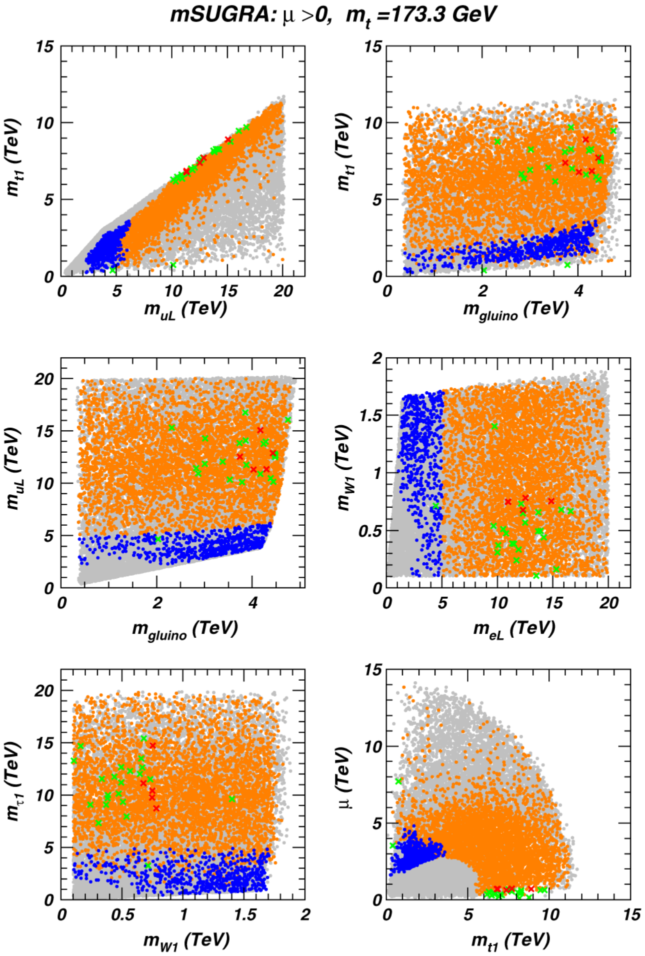

FIG. 7 (color online). Plot of points from general scan over mSUGRA model versus various physical sparticle masses and the μ parameter for $\mu > 0$ with $m_t = 173.3$ GeV. Gray points require neutralino LSP and $m_{\tilde{W}_1} > 103.5$ GeV. Blue and orange points additionally require $m_h = 125 \pm 1$ GeV and have $m_0 < 5$ TeV and 5 TeV $< m_0 < 20$ TeV, respectively. Green and red crosses also require $m_h = 125 \pm 1$ GeV and have the neutralino relic density $\Omega_{\tilde{Z}_1} h^2 < 0.0941$ and $0.0941 < \Omega_{\tilde{Z}_1} h^2 < 0.1277$, respectively.

lighter than 1–2 TeV as well. In Fig. 7(c), we plot $m_{\tilde{q}}$ vs $m_{\tilde{g}}$. Here, we see that the lower-right region, which is the region being currently probed by SUSY searches at LHC, is already excluded if one requires $m_h \sim 125$ GeV. In Fig. 7(d), we plot the values of $m_{\tilde{W}_1}$ vs $m_{\tilde{e}_L}$, the plane which may be relevant for future e^+e^- or $\mu^+\mu^-$ lepton colliders operating in the TeV range. We see that sub-TeV first/second generation sleptons, as favored by the $(g-2)_\mu$ anomaly, are essentially ruled out. However, charginos can have mass as low as $\sim$100 GeV, and so are still a possibility for lepton collider searches. In Fig. 7(e), we show instead the $m_{\tilde{W}_1}$ vs $m_{\tilde{\tau}_1}$ plane. Here, we see that light tau sleptons with mass $m_{\tilde{\tau}_1}$ as low as a few hundred GeV are still allowed provided that $m_{\tilde{W}_1} \gtrsim 0.6$ TeV. Finally, in Fig. 7(f), we show the μ vs $m_{\tilde{t}_1}$ plane. Fine-tuning arguments general favor both low μ and low $m_{\tilde{t}_1}$. Here, we see that the lowest values of μ and $m_{\tilde{t}_1}$ would be essentially ruled out by $m_h \sim 125$ GeV, so that mSUGRA would need to be fine-tuned.

III. IMPLICATIONS OF $m_h = 125$ GeV IN THE NUHM2 MODEL

Since heavy scalar masses are preferred by the rather large value of $m_h = 125$ GeV, we next investigate the NUHM2 model [30], where large values of m_0 need not be limited by the onset of the HB/FP region. The NUHM2 parameter space given by

$$m_0, \quad m_{1/2}, \quad A_0, \quad \tan\beta, \quad \mu, \quad m_A. \tag{3.1}$$

The NUHM2 model parameter space is also closer to what one may expect from SUSY GUT models where the Higgs multiplets live in different GUT representations than the matter multiplets.

Similar to the mSUGRA model described in the previous chapter, we generated 30K random points in the above parameter space, requiring only the radiative EWSB, neutralino LSP, and chargino heavier than 103.5 GeV. Our scan limits are as follows:

$$m_0\colon 0 \to 5 \text{ TeV} \qquad \text{(blue points);}$$
$$m_0\colon 0 \to 20 \text{ TeV} \qquad \text{(orange points),} \tag{3.2}$$

$$m_{1/2}\colon 0 \to 2 \text{ TeV}, \tag{3.3}$$

$$A_0\colon -5m_0 \to +5m_0, \tag{3.4}$$

$$\tan\beta\colon 5 \to 55, \tag{3.5}$$

$$\mu\colon 0 \to 5 \text{ TeV}, \tag{3.6}$$

$$m_A\colon 0 \to 5 \text{ TeV}. \tag{3.7}$$

We only consider positive μ values that are favored by the measurements of the muon anomalous magnetic moment, $(g-2)_\mu$ [20].

Our results in Fig. 8 show the value of m_h generated versus each model parameter. From Fig. 8(a), we see that it is a rather general conclusion that in order to accommodate $m_h \sim 125$ GeV, a rather large value of $m_0 \gtrsim 0.8$ TeV is required. Indeed, this is consistent with early LHC SUSY searches for gluino and squark production, where $m_{\tilde{q}} \sim m_{\tilde{g}} \gtrsim 1$ TeV is already required in gravity-mediated models with gaugino mas unification [27,28]. In Fig. 8(b), we see that no such constraint on $m_{1/2}$ arises, and that essentially the entire range of $m_{1/2}$ can yield a light Higgs scalar h with $m_h \sim 125$ GeV. In Fig. 8(c), we plot m_h versus A_0. If m_0 is limited by 5 TeV, we see that large values of m_h consistent with 125 GeV occur when $A_0 \sim \pm 2m_0$, as noted previously in Ref. [10]. Also, the range $|A_0| \lesssim 1.8m_0$

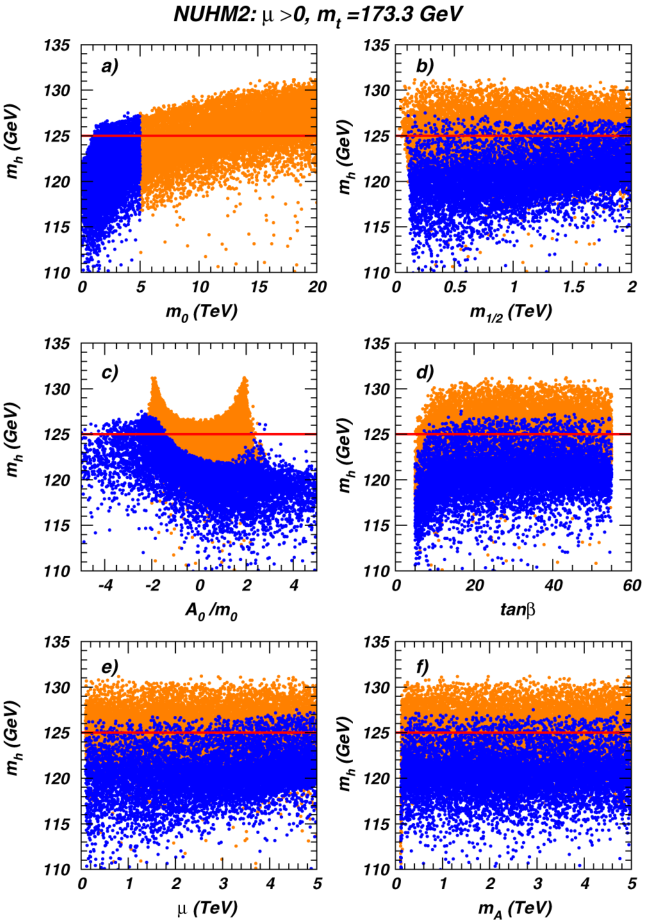

FIG. 8 (color online). Lightest Higgs boson mass versus various SUSY parameters from a scan over NUHM2 parameter space with m_0 up to 5 TeV (blue points) and m_0 up to 20 TeV (orange points). We take positive μ and $m_t = 173.3$ GeV.

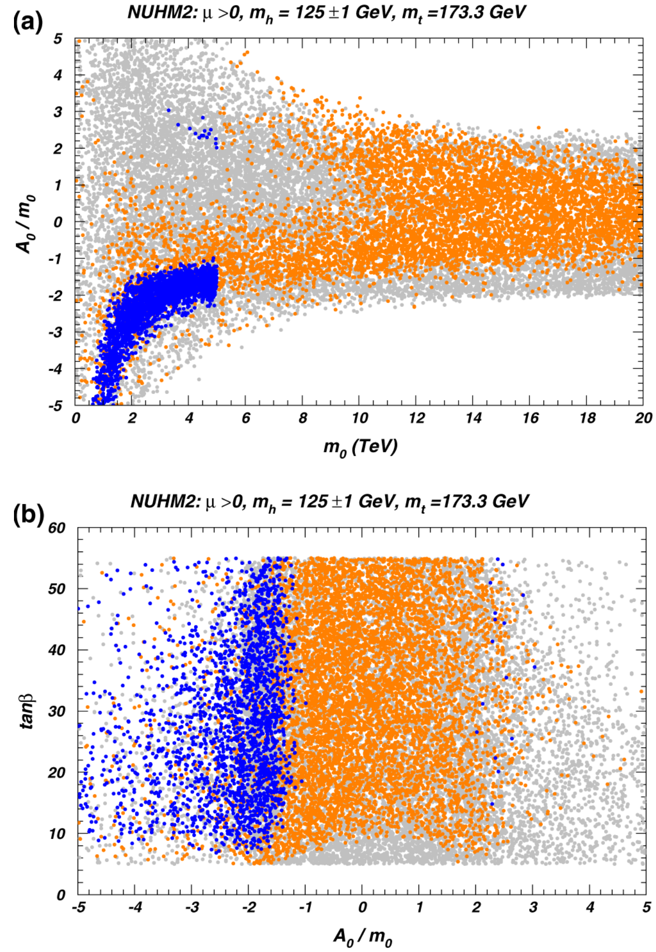

FIG. 9 (color online). Distribution of NUHM2 points with $m_h = 125 \pm 1$ GeV in (a) the m_0 vs A_0/m_0 plane and (b) the A_0/m_0 vs $\tan\beta$ plane. Gray points require neutralino LSP and $m_{\tilde{W}_1} > 103.5$ GeV. Blue and orange points additionally require $m_h = 125 \pm 1$ GeV and have, respectively, $m_0 < 5$ TeV and 5 TeV $< m_0 < 20$ TeV. We take $m_t = 173.3$ GeV.

would be excluded. However, if we extend m_0 up to 20 TeV, as denoted by orange points, then the range $A_0 < 2.5m_0$ is allowed, and only $A_0 \gtrsim 2.5m_0$ is excluded. In Fig. 8(d), we plot m_h versus $\tan\beta$ in NUHM2. Here, we see that almost the entire range of $\tan\beta$ is allowed by requiring $m_h \simeq 125$ GeV, except for very low values $\tan\beta \lesssim 6$ if $m_0 < 5$ TeV. The case where $\tan\beta \sim 50$ includes $t - b - \tau$ Yukawa-unified SUSY [31,32]. In this class of models, one requires very large $m_0 \gtrsim 10$ TeV, low $m_{1/2}$, $A_0 \sim -2m_0$, and split Higgs masses at the GUT scale, with $m^2_{H_u} < m^2_{H_d}$ (at $M_{\rm GUT}$) in order to accommodate radiative electroweak symmetry breaking. This class of models leads to an inverted scalar mass hierarchy [33], wherein third generation scalars exist at sub-TeV values while first/second generation scalars exist at multi-TeV values. The $t - b - \tau$ Yukawa-unified models tend to predict $m_h \gtrsim$ 125 GeV, depending on how high a value of m_0 is allowed.[1] In Figs. 8(e) and 8(f), we plot m_h versus μ and m_A. Here, we find—unlike in the mSUGRA case—no preference for any μ or m_A value in scans with m_0 up to either 5 or 20 TeV if $m_h \simeq 125$ GeV.

We have seen that the existence of a light Higgs scalar h with mass $m_h \simeq 125$ GeV leads to significant constraints on A_0, $\tan\beta$ and m_0. It is then worthwhile to investigate correlations among these parameters when $m_h \simeq 125$ GeV is required. In Fig. 9(a), we show allowed NUHM2 points in the m_0 vs A_0/m_0 plane. Gray colored points allow any value of m_h, while blue points require $m_h = 125 \pm 1$ GeV. Orange points result from extending our scan in m_0 up to 20 TeV. From frame (a), we see that very large values of $m_0 \gtrsim 10$ TeV are preferred by the density of model points. However, some models with $m_h = 125 \pm 1$ GeV can be generated at much lower m_0 values, especially if $A_0 < 0$. In particular, a significant swath of parameter space with $m_0 \lesssim 5$ TeV and $A_0 > 0$ is evidently inconsistent with $m_h \simeq 125$ GeV. In frame (b), we plot the same points in

[1]This is already shown in Fig. 2 of the first paper of Ref. [32]. For a more recent computation, see [34].

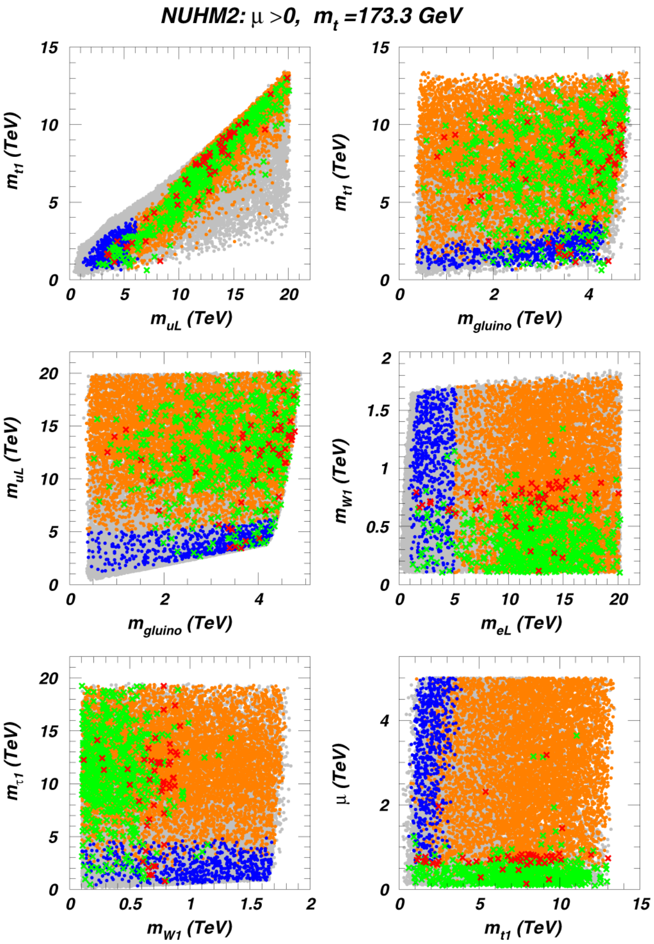

FIG. 10 (color online). Plot of points from general scan over NUHM2 model versus various physical sparticle masses and the μ parameter for $\mu > 0$ with $m_t = 173.3$ GeV. The color coding is the same as in Fig. 7.

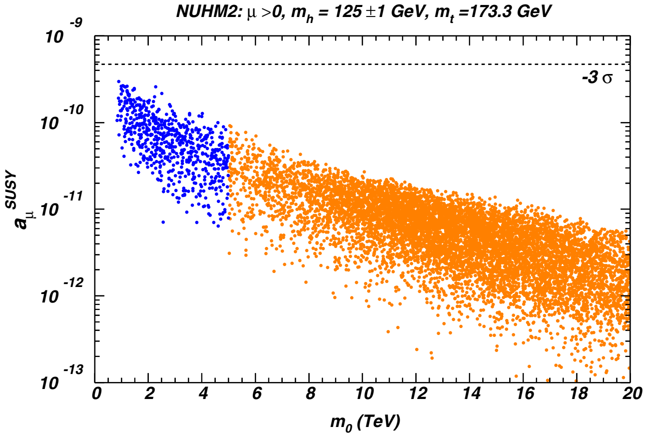

FIG. 11 (color online). Distribution of the SUSY contribution to the muon magnetic moment $a_\mu^{\rm SUSY}$ vs m_0 from scan over NUHM2 parameters restricted by $m_h = 125 \pm 1$ GeV. Blue points denote $m_0 < 5$ TeV, while orange points allow m_0 values up to 20 TeV. The dashed line represents the lower bar of the experimental 3σ range [20].

the A_0/m_0 vs $\tan\beta$ plane. Here, we see that the greatest density of points with $m_h = 125 \pm 1$ GeV occurs for $|A_0/m_0| \lesssim 3$. However, there is an evidently new excluded region of very low A_0 values when $\tan\beta \lesssim 6 - 8$.

In Fig. 10, we plot various physical mass combinations along with the value of the superpotential μ parameter as in Fig. 7. Again, gray points require neutralino LSP and chargino satisfying the LEP2 bound, while blue points additionally require $m_h = 125 \pm 1$ GeV in scans up to $m_0 < 5$ TeV and orange points with m_0 as high as 20 TeV in order to compare with Fig. 7. Green crosses have in addition $\Omega_{\tilde{Z}_1} h^2 < 0.0941$, while red crosses have $.0941 < \Omega_{\tilde{Z}_1} h^2 < 0.1277$. In Fig. 10(a), we see again that rather heavy first/second generation squarks are required, but now $m_{\tilde{q}} \gtrsim 1.5$ TeV, somewhat lower than in mSUGRA. The top squark $\tilde{t}_1$ usually has $m_{\tilde{t}_1} \sim \frac{3}{4} m_{\tilde{q}}$, although it can also range well below this value. In Fig. 10(b), we again see a wide range of $\tilde{t}_1$ and $\tilde{g}$ masses are allowed, with no particular correlation. In Fig. 10(c),—the $m_{\tilde{q}}$ vs $m_{\tilde{g}}$ mass plane, we see that the lower-right region, which was excluded in mSUGRA, now admits some solutions in the NUHM2 model. In Fig. 10(d),—the $m_{\tilde{W}_1}$ vs $m_{\tilde{e}_L}$ plane, we now obtain solutions with $m_{\tilde{\ell}_L}$ as low as $\sim$1 TeV even for the case of light charginos, in contrast to the more constrained mSUGRA model case. In Fig. 10(e), we find that very light, sub-TeV stau particles are allowed, which may give rise to stau coannihilation in the early universe. And finally, in Fig. 10(f),—the μ vs $m_{\tilde{t}_1}$ plane—we are able to generate solutions with low $m_{\tilde{t}_1}$ and low μ, so that the NUHM2 model allows for much less fine-tuning than mSUGRA. We also see the green and red points with thermal neutralino relic density in accord with WMAP measurements, mainly occur at very low μ values, indicating a $\tilde{Z}_1$ of mixed bino-Higgsino variety with a large annihilation cross section in the early universe.

IV. FURTHER IMPLICATIONS OF $m_h = 125$ GeV: RARE DECAYS, $(g-2)_\mu$ AND DARK MATTER SEARCHES

A. $(g-2)_\mu$ and b decays

For $(g-2)_\mu$, we actually calculate $a_\mu^{\rm SUSY}$, i.e. the SUSY contribution [35] to $a_\mu \equiv \frac{(g-2)_\mu}{2}$. In Fig. 11, we plot the value of $a_\mu^{\rm SUSY}$ from our scan over NUHM2 model points with the restriction that $m_h = 125 \pm 1$ GeV. The dashed line represents the lower bar of the 3σ range as extracted by Davier *et al.* in .Ref. [36], where it is found that the discrepancy with the SM is given by $\Delta a_\mu = (28.7 \pm 8.0) \times 10^{-10}$. The central value lies above the plotted range. The main point is that all allowed parameter points with $m_h \sim 125$ GeV are inconsistent with the observed $(g-2)_\mu$ anomaly. This is because a large value of $m_h \sim 125$ GeV favors large m_0 and A_0, which leads to a

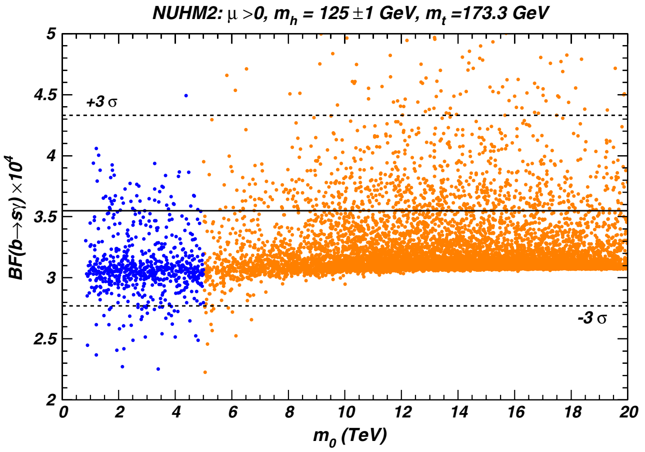

FIG. 12 (color online). Value of $BF(b \to s\gamma)$ vs m_0 from scan over NUHM2 parameters restricted by $m_h = 125 \pm 1$ GeV. Blue points denote $m_0 < 5$ TeV, while orange points allow m_0 values up to 20 TeV. The solid line gives the measured central value and the dashed lines represent the 3σ range [38].

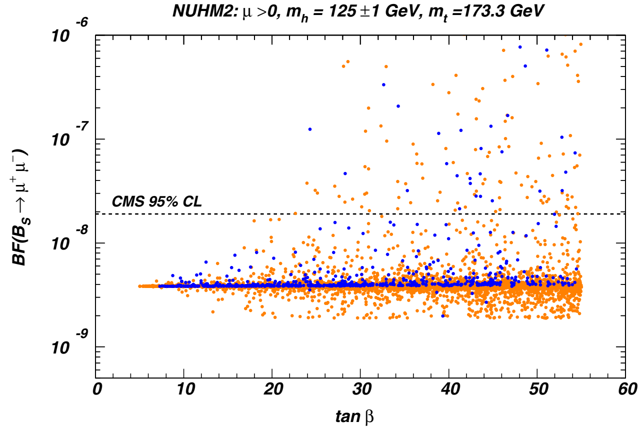

FIG. 13 (color online). Value of $BF(B_s \to \mu^+\mu^-)$ vs $\tan\beta$ from scan over NUHM2 parameters restricted by $m_h = 125 \pm 1$ GeV. Blue points denote $m_0 < 5$ TeV, while orange points allow m_0 values up to 20 TeV. The dashed line represent the 95% C.L. upper limit from the CMS [40].

decoupling of the SUSY contribution to $(g-2)_\mu$. While $m_h \sim 125$ GeV tends to favor high m_0, the discrepancy with the measured value of $(g-2)_\mu$ only increases as m_0 increases.

In Fig. 12, we plot the value of $BF(b \to s\gamma)$ [37] from all SUSY points in NUHM2 parameter space with $m_h = 125 \pm 1$ GeV. For $BF(b \to s\gamma)$, the solid line gives the measured central value and the dashed lines represent the 3σ range from Ref. [38], where $(3.55 \pm 0.26) \times 10^{-4}$ is reported. We see that most NUHM2 points tend to cluster around $BF(b \to s\gamma) \sim 3.1 \times 10^{-4}$, which is the expected SM value. In this case, the large value of m_0 preferred by $m_h \sim 125$ GeV tends to give a decoupling effect, although certainly values of $BF(b \to s\gamma)$ as high as the central value are common.

In Fig. 13, we show the values of the branching fraction $BF(B_s \to \mu^+\mu^-)$ [39] from NUHM2 models with $m_h = 125 \pm 1$ GeV. The dashed line represents the 95% C.L. upper limit from the CMS experiment [40]: $BF(B_s \to \mu^+\mu^-) < 1.9 \times 10^{-8}$. A similar limit from the LHCb experiment [41] gives $BF(B_s \to \mu^+\mu^-) < 1.6 \times 10^{-8}$. The CDF experiment claims evidence for a signal, but still derives a 95% C.L. upper limit $BF(B_s \to \mu^+\mu^-) < 3.9 \times 10^{-8}$ [56]. For illustration, we show the CMS result in the plot. The bulk of points cluster around the SM expectation of 3.2×10^{-9}, which is also the SUSY decoupling limit.

In Fig. 14 we plot the calculated ratio of branching fractions $R_{\tau\nu_\tau} \equiv BF(B_u \to \tau^+\nu_\tau)_{\rm MSSM}/BF(B_u \to \tau^+\nu_\tau)_{\rm SM}$ vs $\tan\beta$ from NUHM2 models with $124\ {\rm GeV} < m_h < 126$ GeV. The SM amplitude for this decay occurs via W-boson exchange, while the MSSM contribution occurs via H^+ exchange [42]. The interference is dominantly negative except at very high $\tan\beta$ and low m_{H^+}. We also show the experimentally-measured central value [43] and the $\pm 2\sigma$ deviation. The bulk of points lie close to the SM-predicted value, while many others exhibit negative interference with $R_{\tau\nu_\tau} < 1$, and some are even excluded. A few points give a positive enhancement in agreement with the measured trend.

B. Implications for neutralino dark matter

Next, we examine implications of $m_h \simeq 125$ GeV for the neutralino dark matter. We calculate the thermal neutralino abundance using ISARED [44], which includes all relevant neutralino annihilation and coannihilation reactions along with relativistic thermal averaging of neutralino (co)-annihilation cross sections times relative velocity. The value of $\Omega_{\tilde{Z}_1}h^2$ is plotted versus $m_{\tilde{Z}_1}$ from NUHM2 model

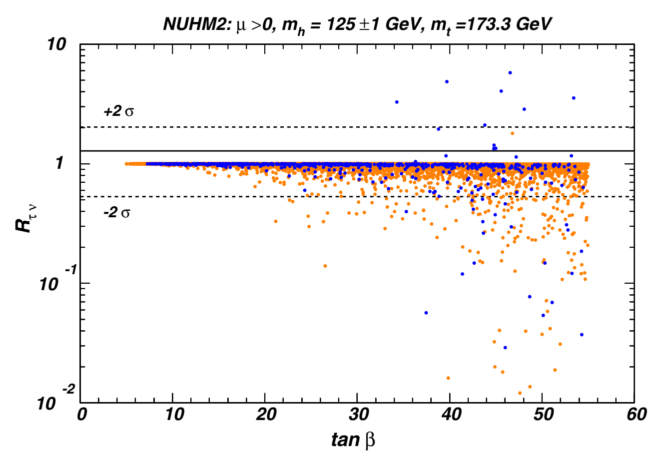

FIG. 14 (color online). Value of $R_{\tau\nu_\tau} \equiv BF(B_u \to \tau^+\nu_\tau)_{MSSM}/BF(B_u \to \tau^+\nu_\tau)_{\rm SM}$ vs $\tan\beta$ from scan over NUHM2 parameters restricted by $m_h = 125 \pm 1$ GeV. Blue points denote $m_0 < 5$ TeV, while orange points allow m_0 values up to 20 TeV. The solid line denotes the central experimental value, while dashed lines represent the $\pm 2\sigma$ error bars [43].

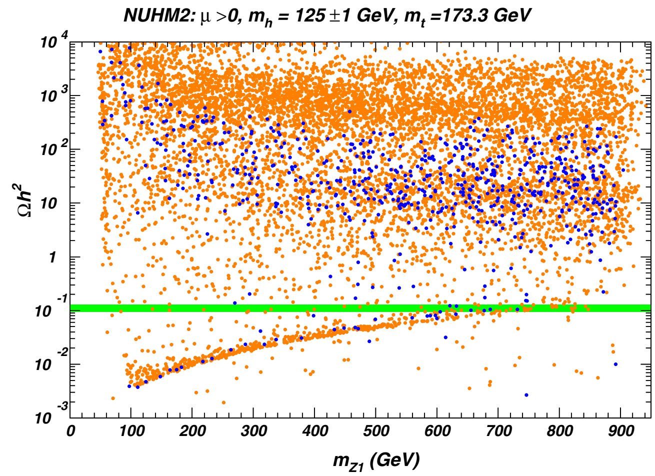

FIG. 15 (color online). Neutralino relic density $\Omega_{\tilde{Z}_1}h^2$ versus the neutralino mass $m_{\tilde{Z}_1}$ from scan over NUHM2 parameters with $m_h = 125 \pm 1$ GeV. Blue points denote $m_0 < 5$ TeV, while orange points allow m_0 values up to 20 TeV. The shaded green horizontal band represents the WMAP 3-σ range [29].

points with $m_h = 125 \pm 1$ GeV in Fig. 15. The WMAP-7 reported the value [29] of $\Omega_{\rm CDM}h^2 = 0.1109 \pm 0.0056$ (68% C.L.) and we plot the 3-σ range as the green band. We see that the bulk of SUSY points with $m_h \simeq 125$ GeV have a large *overabundance* of thermal neutralino dark matter, with $\Omega_{\tilde{Z}_1}h^2 \sim 1 - 10^4$ being typical, so that under a standard cosmology, these points would be excluded. There also exists a lower band crossing $\Omega_{\tilde{Z}_1}h^2 \sim 0.1$ at $m_{\tilde{Z}_1} \sim 0.8$ TeV: this is the case where $\tilde{Z}_1$ is a mixed bino-Higgsino state: it would seem to imply that under a standard cosmology, we would expect a 0.8 TeV Higgsino/bino-like neutralino as the dark matter candidate.

It has been shown in several papers that the presence of a multi-TeV modulus field which decays late and dilutes all relics via entropy injection can bring a large thermal overabundance of neutralino CDM into accord with measurement [45]. Also, the presence of a light axino $\tilde{a}$ (arising from the Peccei-Quinn [46] solution to the strong *CP* problem) can eliminate a neutralino overabundance, since each massive neutralino may decay to a light axino: in this case the relic abundance is reduced by a factor [47] $\frac{m_{\tilde{a}}}{m_{\tilde{Z}_1}}\Omega_{\tilde{Z}_1}h^2$. Then, the remaining dark matter abundance can be built up from axions produced via coherent oscillations [48]. Furthermore, the case of an *underabundance* of light Higgsino-like neutralinos can be boosted by thermal axino production and decay in a scenario with mixed axion/neutralino CDM [49,50].

In Fig. 16, we plot the spin-independent neutralino-proton direct detection cross section versus $m_{\tilde{Z}_1}$ from our scan over NUHM2 models with $m_h = 125 \pm 1$ GeV. We also plot the latest limit from the Xenon-100 collaboration [51]. We see that by far the bulk of points lie below, and most very much below, the current Xenon-100 bound.

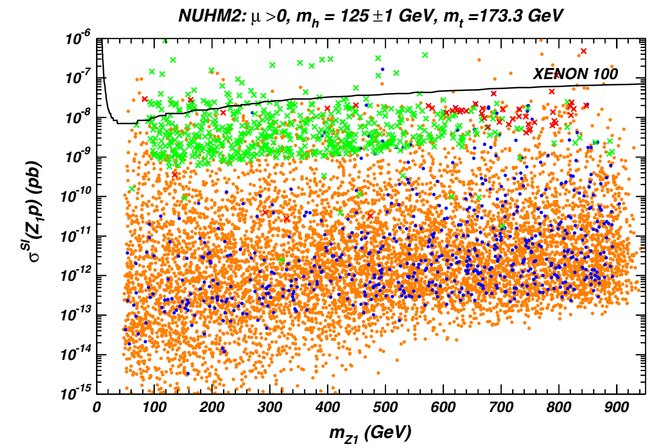

FIG. 16 (color online). Neutralino spin-independent direct detection cross section $\sigma(\tilde{Z}_1 p)$ vs $m_{\tilde{Z}_1}$ from a scan over NUHM2 model points restricted by $m_h = 125 \pm 1$ GeV. Blue points denote $m_0 < 5$ TeV, while orange points allow m_0 values up to 20 TeV. Green and red crosses have the neutralino relic density $\Omega_{\tilde{Z}_1}h^2 < 0.0941$ and $0.0941 < \Omega_{\tilde{Z}_1}h^2 < 0.1277$, respectively. The solid black curve represents the limit from the XENON 100 experiment [51].

Green crosses have in addition $\Omega_{\tilde{Z}_1}h^2 < 0.0941$, while red crosses have $.0941 < \Omega_{\tilde{Z}_1}h^2 < 0.1277$. The green points tend to come from nearly pure Higgsino-like neutralinos with a standard underabundance. In models of mixed axion-$\tilde{Z}_1$CDM, neutralinos with a standard underabundance tend to get an increased abundance from axino and saxion production and decay, so that neutralinos tend to dominate over axions as the main component of CDM. We see that these points tend to cluster around $\sigma(\tilde{Z}_1 p) \sim 10^{-9} - 10^{-8}$ pb as is typical in models with a well-tempered neutralino [52], and would likely be accessible to future runs of direct detection experiments.

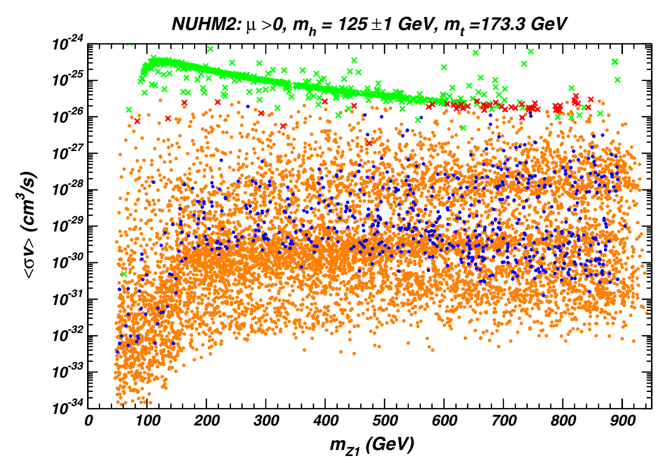

FIG. 17 (color online). Thermally-averaged neutralino annihilation cross section times relative velocity $\langle\sigma v\rangle$ vs $m_{\tilde{Z}_1}$ from scan over NUHM2 points restricted by $m_h = 125 \pm 1$ GeV. The color coding is the same as in Fig. 16.

In Fig. 17, we plot the thermally-averaged neutralino annihilation cross section times relative velocity in the limit as $v \to 0$: $\langle \sigma v \rangle|_{v\to 0}$. This quantity enters estimates of the rate for indirect dark matter detection via observation of gamma rays and antimatter from neutralino annihilation in the galactic halo. Recently, limits have been imposed on this cross section due to the Fermi-LAT collaboration examination of dwarf spheroidal galaxies [53]. We see that models with a standard underabundance—the line of green dots with typically Higgsino-like neutralinos—may ultimately give an observable signal, while models with a standard overabundance tend to have very low annihilation rates, leading to low indirect dark matter detection rates. The green underabundance points—as mixed bino-Higgsino states—tend to annihilate dominantly into WW and ZZ final states.

V. CONCLUSIONS

Evidence has been presented by ATLAS and CMS at the $\sim 2.5\sigma$ level for the existence of a light Higgs scalar with mass $m_h \simeq 125$ GeV. If this evidence is bolstered by an increased data sample in 2012, then the discovery will have strong implications for supersymmetric models. We have examined both the mSUGRA model and the NUHM2 model under the restriction that $m_h = 125 \pm 1$ GeV.

In the case of the mSUGRA (CMSSM) model, we conclude the following.

(i) The common GUT scale scalar mass $m_0 \gtrsim 0.8$ TeV. This tends to imply that squark and slepton masses are >2 TeV with $m_{\tilde{q}} > m_{\tilde{g}}$. In fact, the entire low m_0, low $m_{1/2}$ region of the mSUGRA plane is ruled out independent of A_0 or $\tan\beta$ values.

(ii) The soft breaking trilinear parameter $|A_0| \lesssim 1.8m_0$ is excluded for $m_0 < 5$ TeV, or $|A_0| \lesssim 0.3m_0$ is excluded if m_0 ranges up to 20 TeV.

(iii) The superpotential Higgs mass term $\mu \gtrsim 2$ TeV for $m_0 \lesssim 5$ TeV. This strongly restricts mixed Higgsino-bino states as a source of thermal neutralino CDM, as would be found in the HB/FP region. This constraint is relaxed if m_0 lies in the $5 - 20$ TeV range.

(iv) $m_A \gtrsim 0.8$ TeV, which means $m_{\tilde{Z}_1} \gtrsim 0.4$ TeV if neutralinos annihilate through the A resonance.

In the case of NUHM2 model, we find the following:

(i) $m_0 \gtrsim 0.8$ TeV as in mSUGRA,

(ii) for $m_0 < 5$ TeV, then $A_0 \lesssim -1.8m_0$ or $A_0 \sim +2m_0$,

(iii) for $m_0 \sim 5 - 20$ TeV, then just $A_0 \lesssim 2.5m_0$ is required,

(iv) unlike mSUGRA, the entire ranges of μ and m_A are still allowed,

(v) thermally produced neutralinos match the WMAP-measured relic abundance for a mixed Higgsino state at $m_{\tilde{Z}_1} \sim 0.7$ TeV.

In addition, for NUHM2 and mSUGRA models:

(i) A value of $m_h \simeq 125$ GeV is inconsistent with the $(g-2)_\mu$ anomaly. If the anomaly turns out to be real, it may imply alternative models such as "normal scalar mass hierarchy" [54] where first/second generation GUT scalar masses $m_0(1, 2)$ are much lighter than third generation scalars $m_0(3)$.

(ii) A value of $m_h \simeq 125$ GeV is completely consistent with the measured values of $BF(b \to s\gamma)$, $BF(B_s \to \mu^+\mu^-)$ and $BF(B_u \to \tau^+\nu_\tau)$.

(iii) Neutralino CDM is typically overproduced in the standard MSSM cosmology, unless the neutralino is Higgsino-like, in which case its mass is around 0.8 TeV. In nonstandard cosmologies, such as those including late decaying moduli fields or mixed axion/LSP CDM, the CDM abundance can be easily brought into accord with measured values.

(iv) Direct and indirect WIMP detection rates tend to be very low for models with a standard overabundance of CDM. In the case of Higgsino-like WIMPs with a standard underabundance, direct, and indirect detection prospects are rather bright.

ACKNOWLEDGMENTS

H. B. thanks Jody Brubaker for discussions. This work was supported in part by the U.S. Department of Energy under Grants No. DE-FG02-04ER41305, No. DE-FG02-95ER40896, and No. DE-FG02-94ER-40823.

Note added.— After this work was finished, several papers appeared that also investigated implications of the recent LHC Higgs search results on mSUGRA and NUHM models [55]. Their results tend to agree with ours although small differences do arise due to differences in the considered ranges of model parameters.

[1] ATLAS Collaboration, Report No. ATLAS-CONF-2011-157; CMS Collaboration, Report No. CMS-PAS-HIG-11-023.

[2] F. Gianotti (ATLAS Collaboration), *CERN Public Seminar* (unpublished); ATLAS Collaboration, Report No. ATLAS-CONF-2011-163.

[3] G. Tonelli (CMS Collaboration), *CERN Public Seminar* (unpublished).

[4] R. Barate *et al.* (LEP Working group for Higgs boson searches), Phys. Lett. B **565**, 61 (2003).

[5] For an update, see e.g. J. Erler, Phys. Rev. D **81**, 051301 (2010).

[6] See for example H. Baer and X. Tata, *Weak Scale Supersymmetry: From Superfields to Scattering Events* (Cambridge University Press, Cambridge, England, 2006), p. 184.

[7] H. Haber and R. Hempfling, Phys. Rev. Lett. **66**, 1815 (1991); Y. Okada, M. Yamaguchi, and T. Yanagida, Prog. Theor. Phys. **85**, 1 (1991); J. Ellis, G. Ridolfi, and F. Zwirner, Phys. Lett. B **257**, 83 (1991); **262**, 477 (1991); R. Barbieri and M. Frigeni, Phys. Lett. B **258**, 395 (1991); P. Chankowski, S. Pokorski, and J. Rosiek, Phys. Lett. B **423**, 437 (1994); J. Casas, J. Espinosa, M. Quiros, and A. Riotto, Nucl. Phys. B **436**, 3 (1995); M. Carena, M. Quiros, and C. E. M. Wagner, Nucl. Phys. B **461**, 407 (1996);R. Hempfling and A. H. Hoang, Phys. Lett. B **331**, 99 (1994); R. J. Zhang, Phys. Lett. B **447**, 89 (1999); S. Heinemeyer, W. Hollik, and G. Weiglein, Phys. Rev. D **58**, 091701 (1998); Phys. Lett. B **440**, 296 (1998); Eur. Phys. J. C **9**, 343 (1999); M. Carena, H. Haber, S. Heinemeyer, W. Hollik, C. E. M. Wagner, and G. Weiglein, Nucl. Phys. B **580**, 29 (2000); W. Hollik and D. Stockinger, Phys. Lett. B **634**, 63 (2006); for a review, see e.g. M. Carena and H. Haber, Prog. Part. Nucl. Phys. **50**, 63 (2003).

[8] A. Nisati (ATLAS Collaboration), Lepton-Photon 2011 Meeting, Mumbai, India, Report No. ATLAS-CONF-2011-134 (to be published).

[9] V. Sharma (CMS Collaboration), Lepton-Photon 2011 Meeting, Mumbai, India, Report No. CMS-PAS-HIG-11-014 (to be published).

[10] H. Baer, V. Barger, P. Huang, and A. Mustafayev, Phys. Rev. D **84**, 091701.(2011).

[11] A. Belyaev, Q. H. Cao, D. Nomura, K. Tobe, and C. P. Yuan, Phys. Rev. Lett. **100**, 061801 (2008).

[12] M. A. Bisset, Ph. D thesis, University of Hawaii [Institution Report No. UMI-95-32579, 1994].

[13] D. Pierce, J. Bagger, K. Matchev, and R. J. Zhang, Nucl. Phys. **B491**, 3 (1997).

[14] H. Haber, R. Hempfling, and A. H. Hoang, Z. Phys. C **75**, 539.(1997).

[15] H. Baer, F. Paige, S. Protopopescu, and X. Tata, computer code ISAJET, arXiv:hep-ph/0312045; see also H. Baer, C. H. Chen, R. Munroe, F. Paige, and X. Tata, Phys. Rev. D **51**, 1046 (1995); H. Baer, J. Ferrandis, S. Kraml, and W. Porod, Phys. Rev. D **73**, 015010 (2006).

[16] FeynHiggs, by T. Hahn, S. Heinemeyer, W. Hollik, H. Rzehak, and G. Weiglein, Comput. Phys. Commun. **180** (2009) 1426.

[17] SuSpect, by A. Djouadi, J. L. Kneur, and G. Moultaka, Comput. Phys. Commun. **176**, 426 (2007); SoftSUSY, by B. C. Allanach, computer code SOFTSUSY, Comput. Phys. Commun. **143**, 305 (2002); W. Porod, computer code SPHENO, Comput. Phys. Commun. **153**, 275 (2003).

[18] A. Chamseddine, R. Arnowitt, and P. Nath, Phys. Rev. Lett. **49**, 970 (1982); R. Barbieri, S. Ferrara, and C. Savoy, Phys. Lett. **119B**, 343 (1982); N. Ohta, Prog. Theor. Phys. **70**, 542 (1983); L. Hall, J. Lykken, and S. Weinberg, Phys. Rev. D **27**, 2359 (1983).

[19] M. Lancaster (Tevatron Electroweak Working Group and for the CDF and D0 Collaborations), arXiv:1107.5255.

[20] G. W. Bennett *et al.* (Muon $g-2$ Collaboration), Phys. Rev. D **80**, 052008 (2009).

[21] Joint LEP2 Supersymmetry Working Group, Combined LEP Chargino Results up to 208 GeV, http://lepsusy.web.cern.ch/lepsusy/www/inos_moriond01/charginos_pub.html.

[22] H. Baer, V. Barger, A. Lessa, and X. Tata, J. High Energy Phys. 06 (2010) 102.

[23] H. Baer, X. Tata, and J. Woodside, Phys. Rev. D **45**, 142 (1992); H. Baer, C. H. Chen, F. Paige, and X. Tata, Phys. Rev. D **52**, 2746 (1995); Phys. Rev. D **53**, 6241 (1996); H. Baer, C. H. Chen, M. Drees, F. Paige, and X. Tata, Phys. Rev. D **59**, 055014 (1999); H. Baer, C. Balázs, A. Belyaev, T. Krupovnickas, and X. Tata, J. High Energy Phys. 06 (2003) 054; see also, S. Abdullin and F. Charles, Nucl. Phys. **B547**, 60 (1999); S. Abdullin *et al.* (CMS Collaboration), J. Phys. G **28**, 469 (2002); B. Allanach, J. Hetherington, A. Parker, and B. Webber, J. High Energy Phys. 08 (2000) 017.

[24] K. L. Chan, U. Chattopadhyay, and P. Nath, Phys. Rev. D **58**, 096004 (1998); J. Feng, K. Matchev, and T. Moroi, Phys. Rev. Lett. **84**, 2322 (2000); Phys. Rev. D **61**, 075005 (2000); see also H. Baer, C. H. Chen, F. Paige, and X. Tata, Phys. Rev. D **53**, 6241 (1996); H. Baer, C. H. Chen, M. Drees, F. Paige, and X. Tata, Phys. Rev. D **59**, 055014 (1999); for a model-independent approach, see H. Baer, T. Krupovnickas, S. Profumo, and P. Ullio, J. High Energy Phys. 10 (2005) 020.

[25] M. Dine, A. Kagan, and S. Samuel, Phys. Lett. B **243**, 250 (1990); A. Cohen, D. B. Kaplan, and A. Nelson, Phys. Lett. B **388**, 588 (1996); H. Baer, S. Kraml, A. Lessa, S. Sekmen, and X. Tata, J. High Energy Phys. 10 (2010) 018; D. Feldman, G. Kane, E. Kuflik, and R. Lu, Phys. Lett. B **704**, 56 (2011).

[26] M. Drees and M. Nojiri, Phys. Rev. D **47**, 376 (1993); H. Baer and M. Brhlik, Phys. Rev. D **57**, 567 (1998); H. Baer, M. Brhlik, M. Diaz, J. Ferrandis, P. Mercadante, P. Quintana, and X. Tata, Phys. Rev. D **63**, 015007 (2000); J. Ellis, T. Falk, G. Ganis, K. Olive, and M. Srednicki, Phys. Lett. B **510**, 236 (2001); V. D. Barger and C. Kao, Phys. Lett. B **518**, 117 (2001); L. Roszkowski, R. Ruiz de Austri, and T. Nihei, J. High Energy Phys. 08 (2001) 024; A. Djouadi, M. Drees, and J. L. Kneur, J. High Energy Phys. 08 (2001) 055; A. Lahanas and V. Spanos, Eur. Phys. J. C **23** (2002) 185.

[27] G. Aad *et al.* (ATLAS collaboration), arXiv:1109.6572.

[28] S. Chatrchyan *et al.* (CMS Collaboration), Phys. Rev. Lett. **107**, 221804 (2011).

[29] E. Komatsu *et al.* (WMAP Collaboration), Astrophys. J. Suppl. Ser. **192**, 18 (2011).

[30] J. Ellis, K. Olive, and Y. Santoso, Phys. Lett. B **539**, 107 (2002); J. Ellis, T. Falk, K. Olive, and Y. Santoso, Nucl. Phys. **B652**, 259 (2003); H. Baer, A. Mustafayev, S. Profumo, A. Belyaev, and X. Tata, Phys. Rev. D **71**, 095008 (2005); J. High Energy Phys. 07 (2005) 065, and references therein.

[31] V. Barger, M. Berger, P. Ohmann, and R. J. N. Phillips, Phys. Lett. B **314**, 351 (1993); Phys. Rev. D **49**, 4908 (1994).

[32] H. Baer and J. Ferrandis, Phys. Rev. Lett. **87**, 211803 (2001); T. Blazek, R. Dermisek, and S. Raby, Phys. Rev. Lett. **88**, 111804 (2002); T. Blazek, R. Dermisek, and S. Raby, Phys. Rev. D **65**, 115004 (2002); D. Auto, H. Baer,

C. Balazs, A. Belyaev, J. Ferrandis, and X. Tata, J. High Energy Phys. 06 (**2003**) 023; H. Baer, S. Kraml, S. Sekmen, and H. Summy, J. High Energy Phys. 03 (2008) 056; W. Altmannshofer, D. Guadagnoli, S. Raby, and D. Straub, Phys. Lett. B **668**, 385 (2008); I. Gogoladze, R. Khalid, and Q. Shafi, Phys. Rev. D **79**, 115004 (2009); D. Guadagnoli, S. Raby, and D. M. Straub, J. High Energy Phys. 10 (2009) 059; H. Baer, S. Kraml, and S. Sekmen, J. High Energy Phys. 09 (2009) 005.

[33] J. Feng, C. Kolda, and N. Polonsky, Nucl. Phys. **B546**, 3 (1999); J. Bagger, J. Feng, and N. Polonsky, Nucl. Phys. **B563**, 3 (1999); J. Bagger, J. Feng, N. Polonsky, and R. Zhang, Phys. Lett. B **473**, 264 (2000); H. Baer, P. Mercadante, and X. Tata, Phys. Lett. B **475**, 289 (2000); H. Baer, C. Balazs, M. Brhlik, P. Mercadante, X. Tata, and Y. Wang, Phys. Rev. D **64**, 015002 (2001).

[34] I. Gogoladze, Q. Shafi, and C. S. Un, arXiv:1112.2206.

[35] T. Moroi, Phys. Rev. D **53**, 6565 (1996); **56**, 4424(E) (1997); H. Baer, C. Balazs, J. Ferrandis, and X. Tata, Phys. Rev. D **64**, 035004 (2001).

[36] M. Davier, A. Hoecker, B. Malaescu, and Z. Zhang, Eur. Phys. J. C **71**, 1 (2011).

[37] H. Baer and M. Brhlik, Phys. Rev. D **55**, 4463 (1997); H. Baer, M. Brhlik, D. Castano, and X. Tata, Phys. Rev. D **58**, 015007 (1998).

[38] D. Asner *et al.* (Heavy Flavor Averaging Group), arXiv:1010.1589.

[39] K. Babu and C. Kolda, Phys. Rev. Lett. **84**, 228 (2000); J. K. Mizukoshi, X. Tata, and Y. Wang, Phys. Rev. D **66**, 115003 (2002).

[40] S. Chatrchyan *et al.* (CMS Collaboration), Phys. Rev. D **84**, 052008 (2011).

[41] R. Aaij *et al.* (LHCb Collaboration), Phys. Lett. B **708**, 55 (2012).

[42] W. S. Hou, Phys. Rev. D **48**, 2342 (1993); G. Isidori and P. Paradisi, Phys. Lett. B **639**, 499 (2006); D. Eriksson, F. Mahmoudi, and O. Stal, J. High Energy Phys. 11 (2008) 035.

[43] E. Barberio *et al.* (Heavy Flavor Averaging Group Collaboration), arXiv:0808.1297.

[44] H. Baer, C. Balazs, and A. Belyaev, computer code ISARED; see also J. High Energy Phys. 03 (2002) 042.

[45] T. Moroi and L. Randall, Nucl. Phys. **B570**, 455 (2000); G. Gelmini and P. Gondolo, Phys. Rev. D **74**, 023510 (2006); G. Gelmini, P. Gondolo, A. Soldatenko, and C. Yaguna, Phys. Rev. D **74**, 083514 (2006); B. Acharya, G. Kane, S. Watson, and P. Kumar, Phys. Rev. D **80**, 083529 (2009); G. Arcadi and P. Ullio, Phys. Rev. D **84**, 043520 (2011).

[46] R. Peccei and H. Quinn, Phys. Rev. Lett. **38**, 1440 (1977); Phys. Rev. D **16**, 1791 (1977); S. Weinberg, Phys. Rev. Lett. **40**, 223 (1978); F. Wilczek, Phys. Rev. Lett. **40**, 279 (1978).

[47] L. Covi, J. E. Kim, and L. Roszkowski, Phys. Rev. Lett. **82**, 4180 (1999); L. Covi, H. B. Kim, J. E. Kim, and L. Roszkowski, J. High Energy Phys. 05 (2001) 033.

[48] H. Baer, A. Box, and H. Summy, J. High Energy Phys. 08 (2009) 080.

[49] K.-Y. Choi, J. E. Kim, H. M. Lee, and O. Seto, Phys. Rev. D **77**, 123501 (2008); H. Baer, A. Lessa, S. Rajagopalan, and W. Sreethawong, J. Cosmol. Astropart. Phys. 06 (2011) 031.

[50] H. Baer, A. Lessa, and W. Sreethawong, J. Cosmol. Astropart. Phys. 01 (2012) 036.

[51] E. Aprile *et al.* (Xenon-100 Collaboration), Phys. Rev. Lett. **107**, 131302 (2011).

[52] N. Arkani-Hamed, A. Delgado, and G. Giudice, Nucl. Phys. **B741**, 108 (2006); H. Baer, A. Mustafayev, E. Park, and X. Tata, J. Cosmol. Astropart. Phys. 01 (2007) 017; J. High Energy Phys. 05 (2008) 058.

[53] T. E. Jeltema and S. Profumo, J. Cosmol. Astropart. Phys. 11 (2008) 003; M. Ackermann *et al.* (Fermi-LAT Collaboration), Phys. Rev. Lett. **107**, 241302 (2011); A. Geringer-Sameth and S. M. Koushiappas, Phys. Rev. Lett. **107**, 241303 (2011).

[54] H. Baer, A. Belyaev, T. Krupovnickas, and A. Mustafayev, J. High Energy Phys. 06 (2004) 044.

[55] M. Carena, S. Gori, N. R. Shah, and C. E. M. Wagner, arXiv:1112.3336; S. Akula, B. Altunkaynak, D. Feldman, P. Nath, and G. Peim, Phys. Rev. D **85**, 075001 (2012); M. Kadastik, K. Kannike, A. Racioppi, and M. Raidal, arXiv:1112.3647; O. Buchmueller, R. Cavanaugh, A. De Roeck, M. J. Dolan, J. R. Ellis, H. Flacher, S. Heinemeyer, and G. Isidori *et al.*, arXiv:1112.3564; J. Cao, Z. Heng, D. Li, and J. M. Yang, arXiv:1112.4391.

[56] T. Kuhr *et al.* (CDF Collaboration), in *Proceedings of the 2011 Europhysics Conference on High Energy Physics-HEP 2011, July 21–27, 2011, Grenoble, France* (to be published).